Iranian J Biotech. 2020 January;18(1): e2256 DOI: 10.30498/IJB.2020.129046.2256

Research Article

Modeling, Mutagenesis and *In-silico* Structural Stability Assay of the Model of Superoxide Dismutase of *Lactococcus Lactis* Subsp. *Cremoris* MG1363

Nazanin Gholampour-Faroji[2], Monir-sadat Shakeri[3], Jafar Hemmat[2], Mohammad Rastegar-Moghadam[4], Aliakbar Haddad-Mashadrizeh[1*]

[1] Industrial Biotechnology Research Group, Institute of Biotechnology, Ferdowsi University of Mashhad, Mashhad, Iran
[2] Biotechnology Department, Iranian Research Organization for Science and Technology (IROST). Tehran, Iran
[3] Biotechnology Department, Research Institute of Food Science and Technology. Mashhad, Iran
[4] Structural Biology and Bioinformatics Research Group, Khayam Bioeconomy Institute (KBI), Mashhad, Iran

[*] *Corresponding author:* Aliakbar Haddad-Mashadrizeh, Industrial Biotechnology Research Group, Institute of Biotechnology, Ferdowsi University of Mashhad, Mashhad, Iran. Tel/Fax: +98-5118762227, E-mail: a.haddad@um.ac.ir.

Background: Characterizing the structure and function of superoxide dismutase (SOD), as an antioxidant enzyme providing opportunities for its application in food supplements.
Objectives: In this study, the features of the Manganese-SOD of *Lactococcus lactis* (SDLL), subsp. *cremoris* MG1363, as probiotic bacteria, were determined on the basis of the computational methods.
Materials and Methods: The protein's physicochemical properties and the prediction of its secondary structure were determined via the ProtParam server and the GOR program respectively. Moreover, the 3D structures of the proteins were constructed via the MODELLER on the basis of the homology method and the threading algorithm MUSTER. On the other hand, the structural stability of the models was assayed under the quasi-physiological conditions by the GROMACS program via the GROMOS96 43a1 force field in Linux system. Finally, using the Molecular Docking Studies, the functionality features of the models were predicted through their affinity with the corresponding substrates.
Results: The results revealed the physicochemical properties of the SDLL and a 3D model of a chain of the enzyme being similar to the SOD from the *Bacillus Subtilis* (SDBS). The model of the SDLL was checked for quality control purposes including the Ramachandran plot, the ERRAT and the Verifiy3D. The model was suggestive of the structural stability in quasi-physiological conditions; yet, less than that of the SDBS. Assessing the cause of the instability in the SDLL model was indicative of two unstable regions in the area far from the enzyme's active position, they were considered suitable for mutagenesis. Accordingly, the loop substitution for the corresponding region of SDBS and the deletion of the loop positioned at the C terminal of SDLL resulted in a mutant of SDLL with more stability and appropriate affinity with the corresponding substrate.
Conclusion: In general, the study provides a new model of SDLL with certain thermostable features, and a new mutant with suitable stability and functionality on the basis of the direct mutagenesis being used in different applications.
Keywords: Antioxidant enzymes, food supplements, *thermostability*, direct Mutagenesis

1. Background

Free radicals, including the reactive oxygen species (ROS) and the reactive nitrogen species (RNS), are highly active compounds with the ability of reacting with the biological molecules such as proteins, lipids, nucleic acids, enzymes, and other small molecules, resulting in the loss of cellular functions. The deleterious effects of these compounds are ameliorated through antioxidants. They are capable to neutralize the free radicals by donating one of their own electrons or they can act as scavengers. Therefore, they are regarded as guardians of health. There are some enzymatic- and non-enzymatic anti-oxidation systems in protecting the cells from the free radicals, including the superoxide dismutase (SOD), the glutathione peroxidase and the catalase and ascorbic acid, α-tocopherol, carotenoid, thiolantioxidan and the flavonoids (1). The antioxidant enzymes provide an important line of cellular defense against the free radical damages. Among these enzymes, SOD are a major radical superoxide scavenger due to their distinct ability to catalyze the dismutation of the highly reactive superoxide anions to O_2 and less reactive species H_2O_2. Consequently, they plays an important role in cell protection (2-4). These enzymes are Metallo proteins classified in four isoforms: Manganese SOD (Mn-SOD), iron SOD (Fe-SOD), copper/zinc SOD

(Cu/Zn-SOD), and nickel SOD (Ni-SOD). They can be located in cytosol, chloroplast, mitochondria and extracellular spaces. All these types of enzymes are synthesized in prokaryotic organisms; although the eukaryotes have only Mn-SOD, Fe-SOD and Cu/Zn-SOD. It is demonstrated that Mn-SOD is a major mitochondria isoform in fetal development. Also in this enzyme, polymorphisms have been associated with the increase in the risk of neurodegenerative diseases. Current studies indicate that, as a new mechanism for cancer prevention, Mn-SOD may inhibit the glycolysis. Moreover, SODs have valuable effects on the treatment of inflammatory diseases, burn injuries, protection against UV rays and the reduction of facial wrinkles and hyperpigmentation or depigmentation. As a consequence, they can be used in cosmetics industry (2, 5). In fact, SODs have many potential applications in food preservation, sero-diagnosis of pathogens, cosmetic additives and health-promoting supplements (1, 6). Irrespective of the capacity of the body for the generation of SODs, probiotics can reinforce this capability. As probiotics, the anti-oxidative activities of some lactic acid bacteria (LAB) have been authenticatd in different studies. They are important sources in delivering the enzymatic antioxidants in the gut. The genetically engineered LAB has the anti-inflammatory effects because of expressing SOD or catalase (5). Among these bacteria, *Lactococcus lactis* is widely used as a beneficial bacterium in dairy and meat industry (7). These bacteria naturally produce SOD that is able to provide the oxidative stress resistance. Furthermore, the Mn-SOD production has been reported in some LABs such as *Streptococcus thermophiles*, *Lactococcus lactis* and *Lactobacillus gasseri* (2, 8). Accordingly, the producing organisms of these enzymes might provide an opportunity for reinforcing the antioxidant capacity of the body using the probiotic as well as the prebiotic diets. To achieve the aim, the bioinformatics methods have given rise to the best chance for saving time and cost. Accordingly, the modeling, the molecular dynamic simulation (MD), the proteins docking etc. provide the opportunity for the prediction of the three-dimensional structure of the biological and chemical compounds (9-10), their interactions (11), the biological pathways and even simulating the physiological conditions of these biological pathways (12-15). In this regard, some studies have been reported in relation to the modeling of SODs from different species (3-4, 16-17). Nonetheless, no dataset is currently available on the characteristics of SOD from *Lactococcus (L) lactis* subsp. *cremoris* MG1363. SOD has a wide application in industrial and non-industrial procedures wherein its stability is a major characteristic. Accordingly, to obtain a more stable structure of this enzyme, the *in-silico* molecular tools were used in order to present a model for Mn-SOD of *L. lactis* subsp. *cremoris* MG1363.

2. Objectives

The current study aims to characterize the structure and function of the Manganese-superoxide dismutase of *Lactococcus lactis* providing opportunities for the achievement of an efficient model of the enzyme on the basis of the molecular simulation studies.

3. Material and Methods

3.1. The Retrieval of the Sequence and 3D Structure

The amino acid sequence of the target protein molecule, Mn-SOD in *L. lactis* subsp. *cremoris* MG1363 (accession number: AAA85266.1) was retrieved from the protein dataBank of the National Center for Biotechnology Information database (NCBI/protein, http://www.ncbi.nlm.nih.gov). Moreover, the 3D structure of the ligand were obtained from the Zinc database (http://zinc.docking.org/)(18).

3.2. The Physicochemical Properties of Protein

The ProtParam server (https://web.expasy.org/protparam/) was used for the determination of the physiochemical characteristics of the examined sequence including the molecular weight (MW), the theoretical isoelectric point (pI), the extinction coefficient, the total number of positive and negative residues, the instability index, the aliphatic index, the amino acid composition (%) and the Grand Average hydropathy (GRAVY) (19).

3.3. The Secondary Structure Prediction

The protein's secondary structure was anticipated through the secondary structure prediction method or GOR IV (Garnier- Osguthorpe- Robson) (20). To understand the presence of helices, beta turns and the coils in the protein structure, the GOR analysis was carried out. The GOR method uses the two theoretical information and Bayesian statistics for the prediction of the protein's secondary structure (20). Because of its simple assumptions, the GOR method has conceptual advantage over the other subsequent advanced methods such as PHD, PSIPRED, SPINE-X, and the others as well. While these secondary structural predictive tools depend on the machine learning and are typically black boxes in terms of the principles leading to their predictions, the GOR method's reasoning for arriving at a particular prediction. In some cases, this clarity may

be more significant than the slight loss in accuracy of the GOR algorithm. In addition, the GOR IV algorithm is computationally fast (20).

3.4. The Modeling and the Qualitative Evaluation of the 3D Structure

The BLAST program (https://blast.ncbi.nlm.nih.gov/Blast.cgi) was initially used for selection template. Although the quickest way to search the appropriate templates is to use the simple pairwise sequential alignment methods such as BLAST, the results validate the dominant advantage of profile-profile based methods, which generate models with the average TM-score of 26.5% higher than the sequence-profile methods, and 49.8% higher than the sequence-sequence alignment methods. The TM-score is defined to combine the alignment accuracy and coverage as a unique score (21). On the other hand, to recognize the template proteins containing similar folding structures or structural motifs, the the MUlti-Sources ThreadER (MUSTER) method was used to search the PDB library for the structures having similar sequences and secondary structures with the superoxide dismutase of *L. lactis* (SDLL). Accordingly, the 2RCV with the highest sequence and structural similarity with the target sequence was selected in modeling process. Based on the template structures and the multiple sequence alignment, the 3D structure of SDLL was derived from the ‘‘segment matching’’ or ‘‘coordinate reconstruction’’ approach. Subsequently, the model was constructed by the homology-based software via the MODELLER (https://salilab.org/modeller/), and the threading-based server through the MUSTER (https://zhanglab.ccmb.med.umich.edu/MUSTER/) (9-10). Moreover, the models were evaluated for their structural quality by ERRAT, Verify 3D and Ramachandran plot (https://servicesn.mbi.ucla.edu/SAVES/). The Verify 3D constructs a 3D model profile in which each amino acid residue position is characterized by its environmental score (22). The ERRAT is also used for the verification of the proteins' structures determined by crystallography (23). In addition, the accuracy of the predicted models was evaluated by Ramachandran plot via the RAMPAGE server (24) (http://mordred.bioc.cam.ac.uk/~rapper/rampage.php).

3.5. The Molecular Dynamics Simulation

To assess the structural stability of the native and mutant models, the MD simulation was used. In this regard, the version 4.5.3 of the GROMACS program was applied (25) under the GROMOS96 43a1 force field at the Linux system (26) for 10 ns (Nano seconds). To increase the accuracy, the simulation was repeated three times. Accordingly, for water, the well-tested SPC/E was used (12). The system was neutralized with Na+ as counter ions. Moreover, to minimize the energy of each system and to relax the solvent molecules, the steepest-descent algorithm was carried out. Furthermore, regarding the solvent molecules, the LINCS algorithm (13) was employed to fix the chemical bonds between the atoms of the protein and the SETTLE algorithm (14). On the other hand, to maintain a constant temperature and pressure for the various components during the simulation process, the Berendsen coupling algorithm was used (15). Simulations were used applying the isothermal-isobaric (NPT) ensemble with an isotropic pressure of 1.0 bar. The electrostatic interactions took place using the Particle Mesh Ewald (PME) method (27) with a coulomb cutoff of 1.0 nm. All production simulations were run for 10 ns with a time step of 2 Fs. The simulations were conducted for structures of SDLL, SDBS and mutant at a temperature of 300 k. The RMSD was calculated as a measure of the deviation between the respective Cα atoms of the proteins with respect to the initial structures of the Cα atom, the average was taken over the Cα atoms. In the case of the root mean square fluctuations (RMSF), the average was taken over the time. All simulations were repeated to test the convergence of the results.

3.6. The Molecular Docking Studies

To begin with, based on the literature, the active site of SDLL was determined (28). According to the reports, the manganese ion is located at the active site of each monomer of Mn-SOD, which is stabilized by three histidines (His27, His82 and His168), one aspartic acid (Asp164) and one water molecule (**Fig. 4B**). Subsequently, in order to assay the functionality of the models, the protein-ligand interactions were maintained via the AutoDock Vina (11) and the blind docking approach. In this regard, the grid box parameters were included; size x = 40; size y =40; size z = 40 and center x = 0; center y = 0 and center z = 0. Accordingly, the AutoDock Vina was run several times to get the various docked conformations among the models and the anion superoxide as substrate. For each test compound, ten best poses were created and scored using the AutoDock Vina scoring functions. The interactive features were visualized by PyMOL Molecular Graphics System v.1.3 (Schrodinger, LLC).

4. Results

4.1. The Characteristics of the Sequential Context of SDLL

The sequential analysis of SDLL revealed 450 amino acids in the context of enzyme, with 23.253 kDa in the molecular weight, and 5.03 of isoelectric point. It was

found that L (10.7 %), A (10.2%), E (8.7%), N (7.8 %) as well as O and U (0.0%) are the maximum and the least number of amino acids being present in the sequence of SDLL. Moreover, it was noticed that the number of positively (R+K) and negatively (D+E) charged residues of this enzyme are 17 and 31 respectively. The instability index of the SDLL has been computed at 33.72. Meanwhile, the half-life of this enzyme showed a value more than 10 hrs. Furthermore, the aliphatic as well as the hydropathic indexes of the enzyme are calculated on 80.58 and -0.446 respectively. On the other hand, these analyses reveal that the total residues of SDLL are made up of 26 strands, 91 helices and 89 random coils (**Fig. 1**).

Figure 1. The graphical representation of the secondary structures in the sequential context of SDLL with a different frequency including; The random coil as the most frequent (43.20%), alpha helix (44.17%), and the extended strand as less frequent (12.62%).

4.2. The. Structural Modeling and the Qualitative Assessment of SDLL

The sequential similarity searching has resulted in the revelation of eighteen structures of known proteins in the Protein Data Bank with more than 50% of the sequential similarity to the SDLL. However, the threading approach reveals a closely related sequence with the sequential identity and covering equal to 61% and 100% respectively; from the chain A of SOD of *Bacillus Subtilis* as a suitable template. Subsequently, the SDLL model was built by the MUSTER method (**Fig. 2A**) and passed the quality control procedures. The best model of SDLL revealed the Z score being equal to 26.384, and its Ramchandran plot showed that 85.6 % of the residues are located in the most favorable regions, 11.6 % of them in additional authorized regions, 1.1% of the residues in the generously authorized regions, whereas 1.7% of them are situated in the unauthorized region (**Fig .2B**). On the other hand, the ERRAT score of the model and template being evaluated was equal to 94.444% (**Fig. 2C**) and 96.875%, respectively, which is well within the normal range for a highly qualitatively model. Moreover, the Verify_3D of the model confirmed the structure, so that 100% of the residues had an average of 3D-1D score, larger than 0.2.

4.3. The Thermal Stability of SDLL structure

In order to assess the stability of the structures and to gain an insight into the deviation in the tertiary structure of the models at room temperature (at 300K), the RMSD with respect to the initial structure suggested that the SDBS was more stable than the SDLL (**Fig. 3A**). As is

shown in the figure, the RMSD of Cα atoms of the SDLL at 300 K varied between 0.09 nm to 0.19 nm and those of SDBS varied between 0.08 nm to 0.14 nm. This suggests that the deviation in the three dimensional structure of the SDBS seems as little as of the SDLL with respect to initial structure. On the other hand, the fluctuations in the deviation of residues are monitored by the RMSF of the Cα atoms of the two models (**Fig .3B**). This survey reveals that most of the residues in the two models bear common and similar fluctuations. In addition, the residual fluctuations of the models in question are less in SDBS compared with that of the SDLL. However, in the two structural regions of the SDLL being between 90 103 and 200 206, the residual number significantly differs in fluctuation.

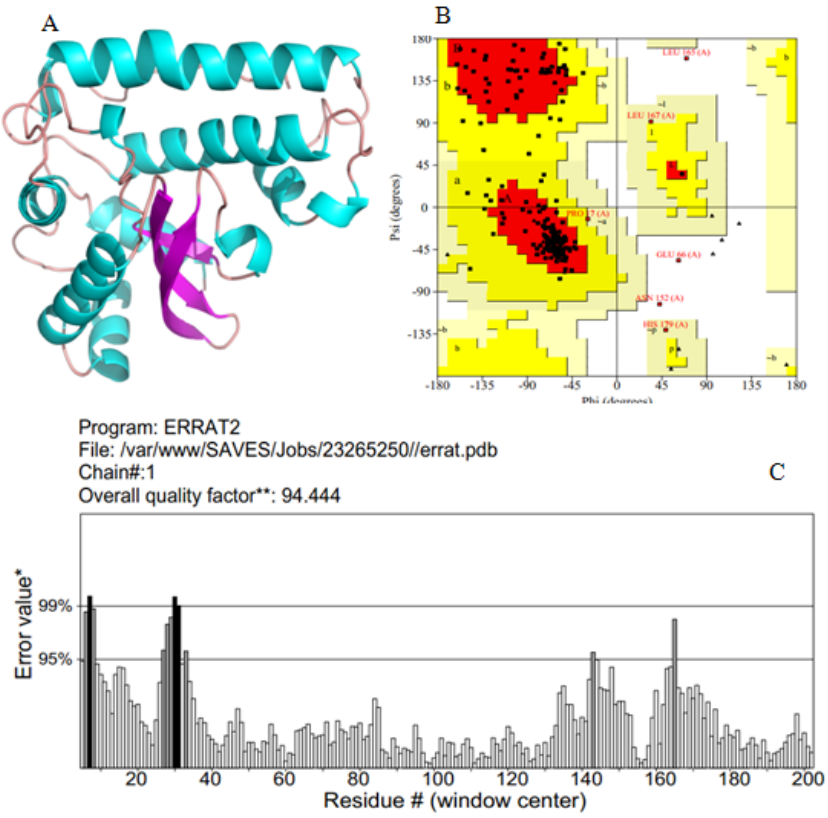

Figure 2. The predictive and the qualitative assay of the 3D structure of SDLL. A) The graphical representation of the best model of the 3D structure of SDLL, B) The position of the residues of SDLL based on the Ramchandran plot, and C) the qualitative features of the model based on the ERRAT curve.

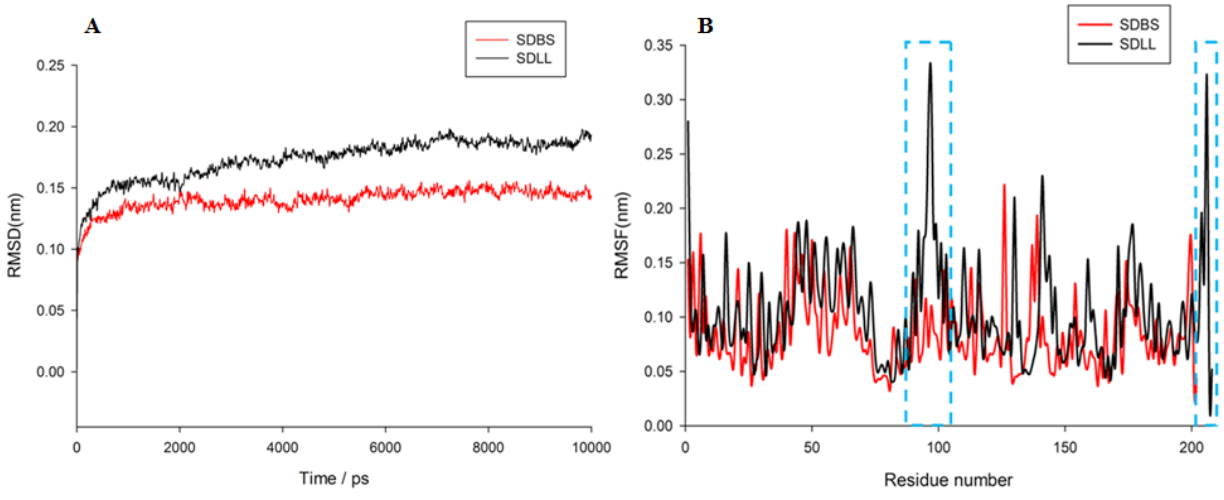

Figure 3. The comparative assay of the thermal stability of the models of SDLL to the SDBS based on A) the RMSD and B) the RMSF curves. The regions with high fluctuations are demonstrated by blue dots in the RMSF curve.

4.5. The Position of the Unstable Structural Regions of SDLL

Probing into the position of the SDLL's unstable regions in the 3D structure of the model has been suggestive of their positions at two loop regions (**Fig. 4**). As is shown in the figure, their locations are on the surface of the model and far from the active-site regions.

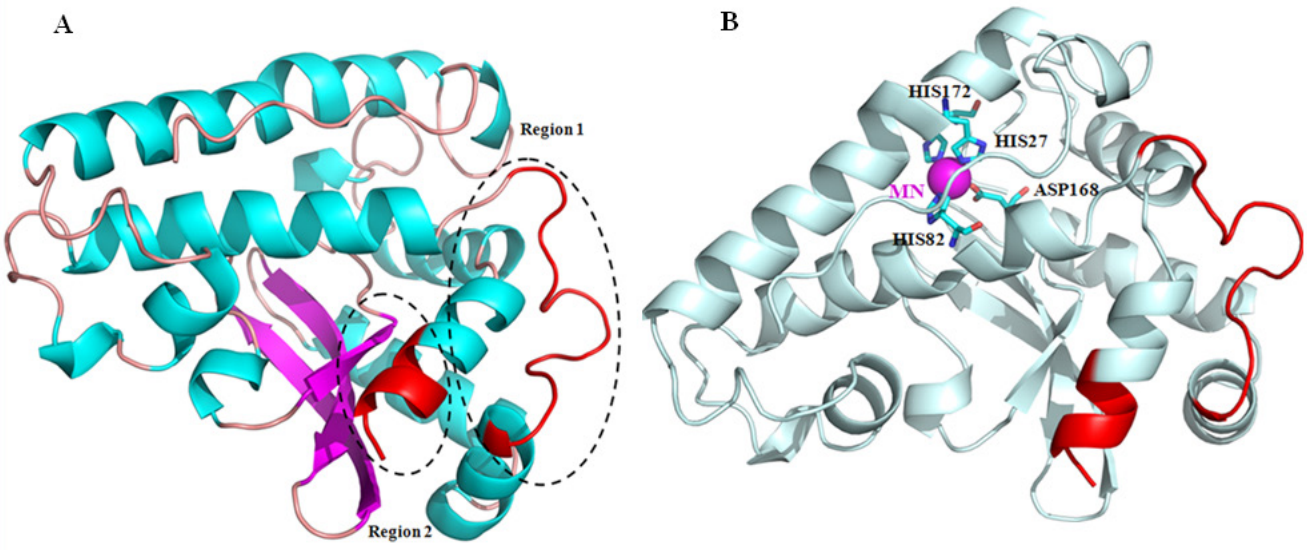

Figure 4. The graphical representation of the unstable regions and the active position of SDLL in the enzyme's 3D structure. A) The unstable regions being restricted via the discontinuous elliptic lines as Region 1 and Region 2. B) The residues of the active site are around the ion-manganese (MN).

4.6. The Characteristics of the Unstable Regions of SDLL

Overlapping the SDLL's 3D structure with that of the SDBS model has led to the discovery of a brief change in length and structure, especially in relation to the region 1 (**Fig. 5**). In this regard, the region 1 at SDLL is a long loop with 13 residues from 90 up to 103, whereas this region at SDBS has 9 residues being located from 92 to 101. On the other hand, the sequential contexts of these regions in the 2 models showed different contexts, so that "PNTDGSENHADGE" are located in the SDLL loop, whereas "PNGGGEPTGAL" are placed in the SDBS loop.

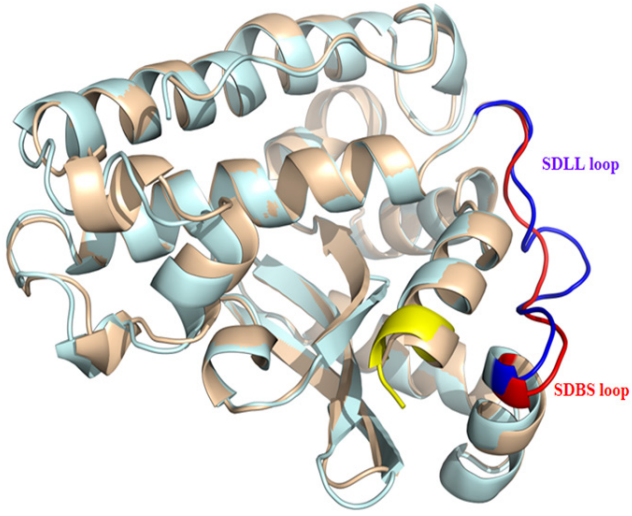

Figure 5. The graphical merge of the structure of SDLL to SDBS.

4.7. The SDLL's Loop Substitution and Deletion

In order to improve the stabilization of SDLL, the modification of its unstable regions was targeted. As to this, the region 1 of the SDLL was substituted short loop of SDBS. Moreover, the unstable region 2 including the LYAKAK residues in the area of 200 to 206 located on the C-terminal of this enzyme was truncated. The mutant with 197 amino acids in length obtained a sequence with different contextual and physicochemical features (**Fig. 6**), without changing in the active position.

4.8 The Functionality and Stability Features of the Mutant of SDLL

The stability and functionality of the mutant were evaluated to assay the effects of mutation on its structure and function. The analysis revealed that compared to the native enzymes the mutations significantly decrease the residual fluctuations (**Fig. 7A**). As is shown in the figure, the mutant residual fluctuations showed more stability, especially in regions 1 and 2 compared to that of the SDLL. While the affinity of the mutant SDLL with the corresponding substrate evaluated -1.5 kcal/mol, the affinity of the SDBS with its substrate was -2.1 kcal/mol. Although the stability of the mutant has increased, its affinity with the substrate (**Fig.7B**) showed less bias compared to that of the SDBS.

```
SDBS        MAYELPELPYAYDALEPHIDKETMTIHHTKHHNTYVTNLNKAVEGNTALANKSVEELVAD
SDLL        MAFTLPELPYAPNALEPFFDEATMRLHHGKHHQTYVNNLNAAIEKHNELDDLSLEELLTD
Mutant      MAFTLPELPYAPNALEPFFDEATMRLHHGKHHQTYVNNLNAAIEKHNELDDLSLEELLTD
            **: ******* :****.:*: ** :** ***:***.*** *:* :. * : *:***::*

SDBS        LDSVPENIRTAVRNNGGGHANHKLFWTLLSPNGGGEP---TGALAEEINSVFGSFDKFKE
SDLL        LSAIPEDIRTAVRNNGGGHLNHSQFWLWLRPNTDGSENHADGEIGDAIAKEFGSFETFKT
Mutant      LSAIPEDIRTAVRNNGGGHLNHSQFWLWLRNGG---GEPTGALIGDAIAKEFGSFETFKT
            *.::**:*********** **. **  *  .          . :.: * . ****:.**

SDBS        QFAAAAAGRFGSGWAWLVVN-NGKLEITSTPNQDSPLSEGKTPILGLDVWEHAYYLNYQN
SDLL        EFKAAATGRFGSGWAWLVVDEAGKLKVVSTANQDNPISEGLTPVLGLDVWEHAYYLKYHN
Mutant      EFKAAATGRFGSGWAWLVVDEAGKLKVVSTANQDNPISEGLTPVLGLDVWEHAYYLKYHN
            :* ***:***********:  ***:.:** ***.*:*** **:***********:*:*

SDBS        RRPDYISAFWNVVNWDEVARLYSERK
SDLL        VRPDYIEAFFNLVNWDKVNELYAKAK
Mutant      VRPDYIEAFFNLVNWDKVNELYAKAK
             *****.**:*:****:* .**:: *
```

Figure 6. The presentation of the sequential context of the SDBS, SBLL and the mutant related to one another based on the multiple alignment. As is shown in here, most of the sequences are similar to one another; however, they are different in loop locations.

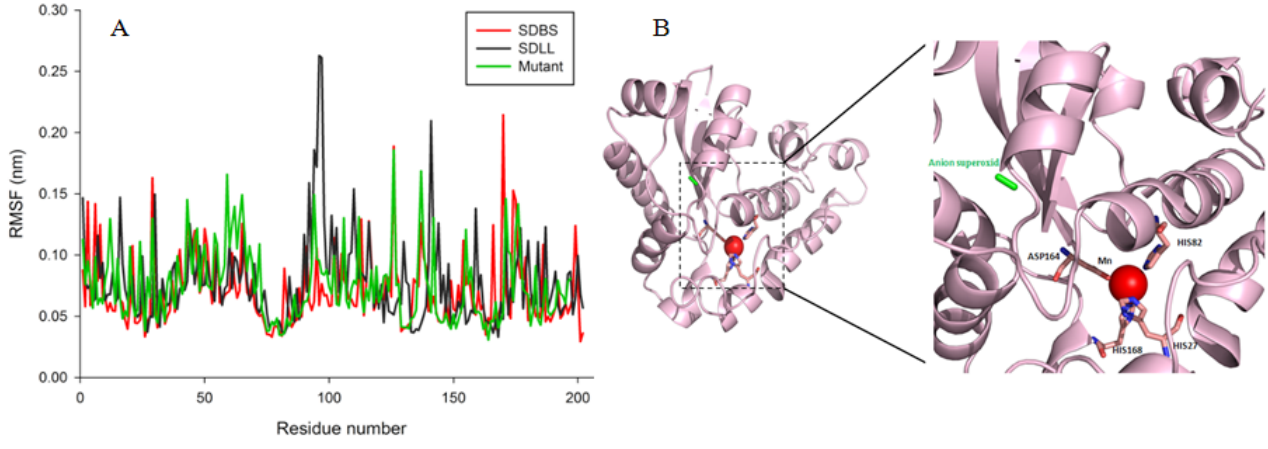

Figure 7. The thermal stability features and the affinity of the mutant with the corresponding substrate. A) The stability of the residues of the mutant compared to the native enzymes based on the RMSF curve. B), the localization of the anion superoxide (Red bullet) as the enzyme's substrate in the active site of the mutant.

5. Discussion:

Protein engineering is an important technology in improving the enzymatic properties used in medical and industrial applications. In this regard, one can already point to many industrial successes. For example, proteases engineered by Genencor (South San Francisco, California, USA) tolerate the bleach in laundry detergents (29). The strategies used in protein engineering including the rational and/or the randomized; however, in each case the desired changes should be applied to the sequential context of the protein. Furthermore, the effects of the mutagenesis on the structure and function of the protein were evaluated via the various methods with different advantages or disadvantages (30). Irrespective of the mutagenesis strategies, the mutant screening could be evaluated via the laboratorial and/ or computational methods. It is rational that the mutagenesis and screening carried out via the *in-silico* approaches before being entered into the laboratorial condition; which are considered

in this study in order to improve the SDLL model properties. Accordingly, the SDLL's sequential features were assessed at the first step. The analysis revealed the enzyme's physicochemical properties. Based on the results obtained, the SDLL with instability index being equal to 33.72 is a stable protein, more than 10 hours in the half-life (31). On the other hand, the aliphatic and hydropathic indexes of the enzyme confirm its thermal stability and water solubility. The Aliphatic Index (AI) which has been defined as the relative volume of a protein occupied by the aliphatic side chains has been regarded as a positive factor for the increase in the thermal stability of the globular proteins (31). So, high AI of the SDLL which is equal to 80.58; indicates the stability of the enzyme in a wide range of temperature conditions (32). Moreover, the very low Grand Average hydropath (GRAVY) index of this enzyme refers to its simple interaction with water (33). Interestingly, in line with these indexes there are 91 helixes in the structure of this enzyme which confirm their stability (34-35). The protein properties such as stability, activity, interface, and size could be changed by the mutagenesis such as N- or C-terminus deletions, the loop deletions and random deletions (36-38). However, in the first place, this operation is completely dependent on the knowledge of the characteristics of each enzyme and protein. Conclusively, the 3D model of the SDLL was built on the basis of its similarity to the sequence of SDBS and which have passed the quality control processes. Predicting the 3D structure of each protein enables the investigator to predict its functions, improve its stability, half-life and its other favorable features (39). Moreover, the thermal stabilities of SDLL and SDBS were evaluated, which revealed unstable regions throughout the SDLL, as suitable candidates for mutagenesis. In this study, the mutant of SDLL was built by substituting and deleting the two unstable regions being between 90-103 and 200-206 residues of the SDLL, with high fluctuations, in a region far from the active position. The substitution took place via the corresponding region of the SDBS's loop, with 9 amino acids in length considered a factor of stability of the SDBS related to the SDLL. The Substitution and the deletion of mutagenesis provide important tools for the alteration of the protein's structures and functions (29). On the other hand, the random evolution and the rational design are two main strategies in protein engineering, which can be combined with the semi-rational design or the focused-directed evolution. The advantage of the randomized pathway is that no structural information is needed and that variations in the unexpected positions distant from the active-site can be introduced (30). Although our strategy was based on the mutagenesis at regions far from the active-site and similar to the directed mutagenesis (30), yet, we used the computational methods as the rational design. In the rational design the biochemical data, the protein structures and the molecular modeling data are evaluated to propose mutations being introduced by the site-specific mutagenesis (30). Moreover, here we used the molecular dynamic simulation (MD) to assess the effects of mutagenesis on the structural stability of the mutant related to the native enzymes. The MD simulation is an effective computational tool to evaluate the proteins' thermostability and flexibility (40), and also to determine the relationship between the structure, the dynamics, and the function of the macromolecules particularly the proteins and other biomolecules. The results of the analysis has been indicative of a significant decrease in the fluctuations of the mutant compared to the native, especially to the SDLL, which refers to the stability of the mutant and confirms our mutagenesis strategy. Considering this, the affinity of the mutant with the corresponding substrate, as an index of its functionality, was evaluated, which confirms the capacity of the mutant to the substrate.

6. Conclusion

Taken as a whole, for the first time, the findings provide a 3D model of superoxide dismutase of *Lactococcus lactis* subsp. *cremoris* MG1363, with a high quality in structure and function. The SDLL model revealed two unstable loops in the area far from the active site of the enzyme. The proposed loop substitution of SDBS and the deletion of the loop positioned in the C terminal of SDLL, may give rise to a mutant SDLL with more stability and suitable affinity with the corresponding substrate. These mutations may improve the enzyme's applications.

Acknowledgement

This work was financially supported and performed at Khayyam Bioeconomy Institute (KBI). The authors are grateful to Amir Moradi for valuable suggestions, as well as to Mohammad-mahdi Esmail-Jami for the editorial and literary editions with respect to the manuscript.

Declarations of interest: We have no conflict of interest to declare.

Reference

1. Krishnamurthy P, Wadhwani A. Antioxidant enzymes and human health. Antioxidant enzyme: *InTech*; 2012. doi: 10.5772/2895.
2. Carroll IM, Andrus JM, Bruno-Bárcena JM, Klaenhammer TR, Hassan HM, Threadgill DS. Anti-inflammatory properties

of Lactobacillus gasseri expressing manganese superoxide dismutase using the interleukin 10-deficient mouse model of colitis. *Am J Physiol Gastrointest Liver Physiol*,. 2007;**293**(4):G729-G738. doi: 10.1152/ajpgi.00132.2007.
3. Ramana Gopavajhula V, Viswanatha Chaitanya K, Akbar Ali Khan P, Shaik JP, Narasimha Reddy P, Alanazi M. Modeling and analysis of soybean (Glycine max. L) Cu/Zn, Mn and Fe superoxide dismutases. *Genet.Mol Biol* 2013;**36**(2):225-236. doi: 10.1590/S1415-47572013005000023.
4. De Carvalho MDC, De Mesquita JF. Structural modeling and in silico analysis of human superoxide dismutase 2. *PloS one*. 2013;**8**(6):e65558.doi: 10.1371/journal.pone.0065558.
5. Bafana A, Dutt S, Kumar S, Ahuja PS. Superoxide dismutase: an industrial perspective. *Crit Rev Biotechnol*. 2011 Mar;**31**(1):6576. doi: 10.3109/07388551.2010.490937. 6. Robbins D, Zhao Y. Manganese superoxide dismutase in cancer prevention. Antioxidants & redox signaling. 2014;**20**(10):1628-1645.
7. Del Carmen S, de Moreno de LeBlanc A, Martin R, Chain F, Langella P, Bermudez-Humaran LG, *et al*. Genetically engineered immunomodulatory Streptococcus thermophilus strains producing antioxidant enzymes exhibit enhanced anti-inflammatory activities. *Appl Environ Microbio*l. 2014 Feb;**80**(3):869-877. doi: 10.1128/AEM.03296-13.
8. Lee N-K, Han KJ, Son S-H, Eom SJ, Lee S-K, Paik H-D. Multifunctional effect of probiotic Lactococcus lactis KC24 isolated from kimchi. LWT. *Food Sci Technolog*. 2015;**64**(2):1036-1041. doi: 10.1016/j.lwt.2015.07.019.
9. Wu S, Zhang Y. MUSTER: improving protein sequence profile–profile alignments by using multiple sources of structure information. Proteins: Structure, *Function, Bioinformatics*. 2008;**72**(2):547-556. doi: 10.1002/prot.21945.
10. Eswar N, Eramian D, Webb B, Shen MY, Sali A. Protein structure modeling with MODELLER. *Methods Mol Biol*. 2008;**426**:145-159. doi: 10.1007/978-1-60327-058-8_8.
11. Trott O, Olson AJ. AutoDock Vina: improving the speed and accuracy of docking with a new scoring function, efficient optimization, and multithreading. *J Comput Chem*. 2010 Jan 30;**31**(2):455-461. doi: 10.1002/jcc.21334.
12. Hermans J, Berendsen HJ, Van Gunsteren WF, Postma JP. A consistent empirical potential for water–protein interactions. *Comput Biol Chem*.. 1984;**23**(8):1513-1518. doi: 10.1002/bip.360230807
13. Hess B, Bekker H, Berendsen HJ, Fraaije JG. LINCS: a linear constraint solver for molecular simulations. *J Comput Chem*. 1997;**18**(12):1463-1472. doi: 10.1002/(SICI)1096987X(19970 9)18:12<1463::AID-JCC4>3.0.CO;2-H.
14. Miyamoto S, Kollman PA. Settle: An analytical version of the SHAKE and RATTLE algorithm for rigid water models. *J Comput Chem*. 1992;**13**(8):952-962. doi: 10.1002/jcc.540130805.
15. Berendsen HJ, Postma Jv, van Gunsteren WF, DiNola A, Haak J. Molecular dynamics with coupling to an external bath. *J Chem phys*. 1984;**81**(8):3684-3690. doi: 10.1063/1.448118.
16. Buerk DG, Lamkin-Kennard K, Jaron D. Modeling the influence of superoxide dismutase on superoxide and nitric oxide interactions, including reversible inhibition of oxygen consumption. *Free Radic Biol Med*. 2003 Jun 1;**34**(11):14881503. doi: 10.1016/S0891-5849(03)00178-3
17. Pathak R, Narang P, Chandra M, Kumar R, Sharma PK, Gautam HK. Homology modeling and comparative profiling of superoxide dismutase among extremophiles: exiguobacterium as a model organism. *Indian J Microbiol.* 2014 Dec;**54**(4):450458. doi: 10.1007/s12088-014-0482-8
18. Irwin JJ, Shoichet BK. ZINC--a free database of commercially available compounds for virtual screening. *J Chem Inf Model*. 2005 Jan-Feb;**45**(1):177-182. doi: 10.1021/ci049714+.
19. Walker JM. The proteomics protocols handbook: *Springer*; 2005. doi: 10.1385/1592598900.
20. Kouza M, Faraggi E, Kolinski A, Kloczkowski A. The GOR Method of Protein Secondary Structure Prediction and Its Application as a Protein Aggregation Prediction Tool. *Methods Mol Biol*. 2017;**1484**:7-24. doi: 10.1007/978-1-4939-6406-2_2.
21. Yan R, Xu D, Yang J, Walker S, Zhang Y. A comparative assessment and analysis of 20 representative sequence alignment methods for protein structure prediction. *Sci Reports*. 2013;**3**:2619. doi: 10.1038/srep02619.
22. Eisenberg D, Luthy R, Bowie JU. VERIFY3D: assessment of protein models with three-dimensional profiles. *Meth Enzymol.* 1997;**277**:396-404. doi: 10.1016/S0076-6879(97)77022-8.
23. Lüthy R, Bowie JU, Eisenberg D. Assessment of protein models with three-dimensional profiles. Nature. 1992;356(6364):83.
24. Lovell SC, Davis IW, Arendall III WB, De Bakker PI, Word JM, Prisant MG, *et al*. Structure validation by Cα geometry: ϕ, ψ and Cβ deviation. Proteins: Structure, *Fun Bioinformatics*. 2003;**50**(3):437-450. doi: 10.1002/prot.10286.
25. Hess B, Kutzner C, van der Spoel D, Lindahl E. GROMACS 4: Algorithms for Highly Efficient, Load-Balanced, and Scalable Molecular Simulation. *J Comput Chem*. 2008 Mar;**4**(3):435447. doi: 10.1021/ct700301q
26. Daura X, Mark AE, Van Gunsteren WF. Parametrization of aliphatic CHn united atoms of GROMOS96 force field. *J Comput Chem*. 1998;**19**(5):535-547. doi: 10.1002/(SICI)10969 87X(19980415)19:5<535::AID-JCC6>3.0.CO;2-N
27. Darden T, York D, Pedersen L. Particle mesh Ewald: An N. log (N) method for Ewald sums in large systems. *J Chem phys*. 1993;**98**(12):10089-10092. doi: 10.1063/1.464397.
28. Liu P, Ewis H, Huang Y-J, Lu C-D, Tai P, Weber IT. Structure of Bacillus subtilis superoxide dismutase. Acta Crystallographica Section F: *Str Biol Crystallization Communicat*. 2007;**63**(12):10031007. doi: 10.1107/S1744309107054127
29. Kazlauskas RJ, Bornscheuer UT. Finding better protein engineering strategies. *Nat Chem Biol*. 2009;**5**(8):526-529. doi: 10.1038/nchembio0809-526
30. Chica RA, Doucet N, Pelletier JN. Semi-rational approaches to engineering enzyme activity: combining the benefits of directed evolution and rational design. *Curr Opin Biotech*. 2005;**16**(4):378-384. doi : 10.1016/j.copbio.2005.06.004
31. Ikai A. Thermostability and aliphatic index of globular proteins. *J Biochem*. 1980 Dec;**88**(6):1895-1898. doi: 10.1093/oxfordjournals.jbchem.a133168.
32. Guruprasad K, Reddy BV, Pandit MW. Correlation between stability of a protein and its dipeptide composition: a novel approach for predicting in vivo stability of a protein from its primary sequence. *Protein Eng*. 1990 Dec;**4**(2):155-161. doi: 10.1093/protein/4.2.155.
33. Kyte J, Doolittle RF. A simple method for displaying the hydropathic character of a protein. *J.Mol Biol*. 1982;**157**(1):105132. doi: 10.1016/0022-2836(82)90515-0.
34. Abrusán G, Marsh JA. Alpha helices are more robust to mutations than beta strands. *PLoS computational biolog*. 2016;**12**(12):e1005242. doi: 10.1371/journal.pcbi.1005242
35. Rocklin GJ, Chidyausiku TM, Goreshnik I, Ford A, Houliston

S, Lemak A, *et al*. Global analysis of protein folding using massively parallel design, synthesis, and testing. *Sci*. 2017;**357**(6347):168-175. doi: 10.1126/science.aan0693.

36. Gong R, Wang Y, Feng Y, Zhao Q, Dimitrov DS. Shortened engineered human antibody CH2 domains increased stability and binding to the human neonatal Fc receptor. *J Biol Chem*. 2011;**286**(31):27288-27293. doi: 10.1074/jbc.M111.254219.
37. Liu L, Zhang G, Zhang Z, Wang S, Chen H. Terminal amino acids disturb xylanase thermostability and activity. *J Biol Chem*. 2011;**286**(52):44710-44715. doi: 10.1074/jbc.M111.269753.
38. Haglund E, Danielsson J, Kadhirvel S, Lindberg MO, Logan DT, Oliveberg M. Trimming Down a Protein Structure to Its Bare Foldons SPATIAL ORGANIZATION OF THE COOPERATIVE UNIT. *J Biol Chem*. 2012;**287**(4):2731-278. doi: 10.1074/jbc.M111.312447.
39. Webb B, Sali A. Comparative protein structure modeling using Modeller. *Curr Protoc Bioinformatics*. 2014:**5**.6. 1-5.6. 32. doi: 10.1002/0471250953.bi0506s47.
40. Kundu S, Roy D. Structural analysis of Ca 2+ dependent and Ca 2+ independent type II antifreeze proteins: A comparative molecular dynamics simulation study. *J Mol Graph Model*. 2012;**38**:211-219. doi:10.1016/j.jmgm.2012.05.004.